Inorg. Chem. **2007**, *46*, 6099–6107

Inorganic Chemistry

Article

# Synthesis, Structure, and Properties of a Mixed-Valent Triiron Complex of Tetramethyl Reductic Acid, an Ascorbic Acid Analogue, and Its Relationship to a Functional Non-Heme Iron Oxidation Catalyst System

**YooJin Kim, Xudong Feng, and Stephen J. Lippard***

*Department of Chemistry, Massachusetts Institute of Technology, Cambridge, Massachusetts 02139*

Received April 1, 2007

The purple triiron(II,III,III) complex, $[Fe_3Cl_2(TMRASQ)_4(HTMRA)_2]\cdot C_5H_{12}$ ($\mathbf{1}\cdot C_5H_{12}$), where $H_2TMRA$ is a tetramethyl reductic acid, 4,4,5,5-tetramethyl-2,3-dihydroxy-2-cyclopenten-1-one, and HTMRASQ is the semiquinone form of this ligand, was prepared from $(Et_4N)_2[Fe_2OCl_6]$ and $H_2TMRA$ and characterized by X-ray crystallography, Mössbauer spectroscopy, and redox titrations. The physical properties of the complex in solution are consistent with its mixed-valent character, as delineated by a solid-state structure analysis. Assignments of the iron and ligand oxidation states in the crystal were made on the basis of a valence bond sum analysis and the internal ligand geometry. As the first well-characterized iron complex of an ascorbic acid $H_2AA$ analogue, **1** provides insight into the possible coordination geometry of the family of complexes containing $H_2AA$ and its analogues. In the presence of air and $H_2TMRA$, **1** is able to catalyze the oxidation of cyclohexane to cyclohexanol with remarkable selectivity, but the nature of the true catalyst remains unknown.

## Introduction

L-Ascorbic acid ($H_2AA$ in Scheme 1; vitamin C) is used pharmaceutically to counteract scurvy and in the food industry as an antioxidant.[1−5] The coordination chemistry of ascorbic acid with metal ions such as iron and copper is of interest because of its many important biological functions.[6,7] Very few metal complexes of vitamin C (L-ascorbic acid)[7−9] have been structurally characterized, however. Ferrous ion forms a complex with $H_2AA$ in aqueous solution at pH 9[10] that has absorption maxima at 380 and 500 nm. The isolation of purple species formed in the reaction of ferric chloride and ascorbic acid was subsequently reported.[11]

**Scheme 1**

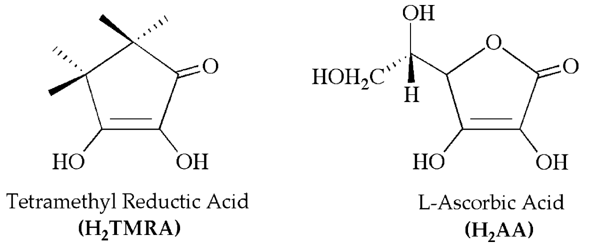

Polymeric and mixed-valent iron $AA^{2-}$ complexes have been described,[12,13] but a definitive structural study has not been forthcoming. Additional kinetic studies of the oxidation of $H_2AA$ catalyzed by ferric species led to a mononuclear iron AA complex, for which the structure depicted in Scheme 2 was proposed.[14,15] A "polynuclear mixed-valent compound" formed between iron and $H_2AA$ was suggested based on

---

* To whom correspondence should be addressed. E-mail: lippard@mit.edu.

(1) Hallberg, L. In *Vitamin C (Ascorbic acid)*; Counsell, J. N., Hornig, D. H., Eds.; Applied Science: London, 1981; pp 49−61.

(2) Gorman, J. E.; Clydesdale, F. M. *J. Food Sci.* **1983**, *48*, 1217−1220.

(3) Jacobsen, C.; Timm, M.; Meyer, A. S. *J. Agric. Food Chem.* **2001**, *49*, 3947−3956.

(4) Kitano, K.; Fukukawa, T.; Ohtsuji, Y.; Masuda, T.; Yamaguchi, H. *Food Chem. Toxicol.* **2002**, *40*, 1589−1594.

(5) Zenki, M.; Tanishita, A.; Yokoyama, T. *Talanta* **2004**, *64*, 1273−1277.

(6) Davies, M. B. *Polyhedron* **1992**, *11*, 285−321.

(7) Zümreoglu-Karan, B. *Coord. Chem. Rev.* **2006**, *250*, 2295−2307.

(8) Hughes, D. L. *J. Chem. Soc., Dalton Trans.* **1973**, 2209−2215.

(9) Kriss, E. E. *Russ. J. Inorg. Chem.* **1978**, *23*, 1004−1008.

(10) Stolyarov, K. P.; Amantova, I. A. *Talanta* **1967**, *14*, 1237−1244.

(11) Conrad, M. E.; Schade, S. G. *Gastroenterology* **1968**, *55*, 35−45.

(12) Jabs, W.; Krüger, G.; Trautwein, A. X.; Schünemann, V.; Bill, E. In *Transition Metals in Biology and Their Coordination Chemistry*; Trautwein, A. X., Ed.; Wiley: Weinheim, Germany, 1997; pp 468−475.

(13) Rao, C. P.; Geetha, K.; Raghavan, M. S. S.; Sreedhara, A.; Tokunaga, K.; Yamaguchi, T.; Jadhav, V.; Ganesh, K. N.; Krishnamoorthy, T.; Ramaiah, K. V. A.; Bhattacharyya, R. K. *Inorg. Chim. Acta* **2000**, *297*, 373−382.

(14) Taqui Khan, M. M.; Martell, A. E. *J. Am. Chem. Soc.* **1967**, *89*, 4176−4185.

(15) Taqui Khan, M. M.; Martell, A. E. *J. Am. Chem. Soc.* **1967**, *89*, 7104−7111.

10.1021/ic700622a CCC: $37.00

**Scheme 2**

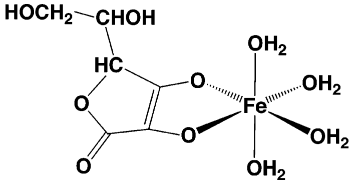

**Scheme 3.** Proton and Different Oxidation States of TMRA

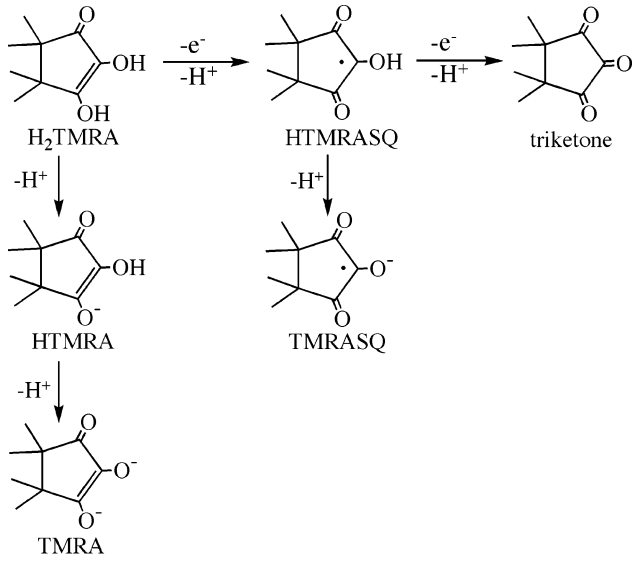

UV−vis and redox potential measurements.[16] Despite these efforts, after many decades the nature and coordination geometry of iron bound to ascorbic acid remain obscure.

Interest in iron ascorbate chemistry was aroused in our laboratory about 20 years ago when it was discovered that the simple dinuclear ($\mu$-oxo)hexachlorodiiron(III) complex, $[Fe_2OCl_6]^{2-}$, together with a suitable reductant such as $H_2AA$ or its analogue $H_2TMRA$ (Scheme 1), was capable of catalyzing the air oxidation of alkanes to alcohols with high selectivities in various solvents.[17−19] The catalytic activity was preceded by the formation of a purple species, possibly the catalyst itself or an immediate precursor, formed between the iron(III) salt and $H_2AA$ or the related $H_2TMRA$ analogue. We therefore set out to isolate and characterize this purple species as a first step toward unraveling the mechanism of the catalytic reaction. The task of crystallizing an iron AA complex proved to be very difficult because the AA complex had a short lifetime in aqueous solution and was insoluble in most nonaqueous solvents. The TMRA analogue had greater solubility in nonpolar solvents such as pentane and hexane. An additional difficulty arose because of various possible redox states of the AA and TMRA ligands (Scheme 3), which provide a variety of electronic and geometric possibilities for coordination to iron.[18] It is possible to distinguish between the semiquinone and reduced forms of these molecules by using single-crystal X-ray crystallography,[20−25] but at the time our instrumentation and/or crystal quality was not up to the task.

Recently we returned to the problem with a CCD diffractometer and have now solved the nature of the ligand valence localization. Here we report the structure and spectroscopic properties of the purple complex $[Fe_3Cl_2(TMRASQ)_4(HTMRA)_2]{\cdot}C_5H_{12}$ ($\mathbf{1}{\cdot}C_5H_{12}$), a mixed-valent $Fe^{III}{}_2Fe^{II}$ complex containing both semiquinone (TMRASQ) and fully reduced (TMRA) coordination. We also present extensive physical characterization data that reveal **1** to have this structure in solution. Compound **1** is catalytically active in the selective oxidation of a variety of hydrocarbons to the corresponding alcohols but is not as proficient as the mixture of $H_2TMRA$ and $(Et_4N)_2[Fe_2OCl_6]$ from which it was prepared. The combination of mixed metal and ligand valence states for **1** is remarkable and likely to be encountered in the coordination chemistry of ascorbic acid and its analogues with redox-active transition-metal ions. Some of these results were reported in preliminary form elsewhere.[19]

## Experimental Section

**General Considerations**. All reagents were obtained from commercial suppliers and used as received unless otherwise noted. The tetramethyl reductic acid was obtained as a gift from Polaroid Corp. Diethyl ether, acetonitrile, and pentane were saturated with argon and purified by passage through activated $Al_2O_3$ columns under argon. The starting material, $(Et_4N)_2[Fe_2OCl_6]$, was prepared as described in the literature.[26] All syntheses and air-sensitive manipulations were carried out under nitrogen in a glovebox or by using standard Schlenk techniques.

**Physical Measurements.** The crystals of $\mathbf{1}{\cdot}C_5H_{12}$ were ground to a fine powder and dried under vacuum for at least 24 h before sending the sample out for elemental analysis or performing any physical measurement. All measurements were carried out anaerobically. FT-IR spectra were obtained on an Avatar 360 spectrometer. UV−vis spectra were recorded on a Hewlett-Packard 8453 diode array spectrophotometer. Mössbauer spectra for both solid and solution samples of **1** were recorded by Dr. Georgia Papaefthymiou at the Francis Bitter Magnet Laboratory at 4.2 and 80 K with zero applied magnetic field.

**Synthesis of $[Fe_3Cl_2(TMRASQ)_4(HTMRA)_2]{\cdot}C_5H_{12}$ ($\mathbf{1}{\cdot}C_5H_{12}$).** To a solution of 300 mg (0.5 mmol) of $(Et_4N)_2[Fe_2OCl_6]$ in 10 mL of $CH_3CN$ was added 170 mg (1.0 mmol) of $H_2TMRA$ in the drybox. The reaction was stirred for 1 h, at which point the solution color was purple. The mixture was filtered through Celite, the solvent was removed under vacuum, and the residue was extracted into ether. The resulting purple solution was then removed from

---

(16) Kurbatova, G. T.; Kriss, E. E.; Grigor'eva, A. S. *Russ. J. Inorg. Chem.* **1981**, *26*, 982−984.

(17) Roth, M. E. Ph.D. Dissertation, Massachusetts Institute of Technology: Cambridge, MA, 1988.

(18) Feng, X. Ph.D. Dissertation, Massachusetts Institute of Technology: Cambridge, MA, 1991.

(19) Rosenzweig, A. C.; Feng, X.; Lippard, S. J. In *Applications of Enzyme Biotechnology*; Kelly, J. W., Baldwin, T. O., Eds.; Plenum Press: New York, 1991; pp 69−85.

(20) Ghosh, P.; Begum, A.; Bill, E.; Weyhermüller, T.; Wieghardt, K. *Inorg. Chem.* **2003**, *42*, 3208−3215.

(21) Shaikh, N.; Goswami, S.; Panja, A.; Wang, X.-Y.; Gao, S.; Butcher, R. J.; Banerjee, P. *Inorg. Chem.* **2004**, *43*, 5908−5918.

(22) Buchanan, R. M.; Kessel, S. L.; Downs, H. H.; Pierpont, C. G.; Hendrickson, D. N. *J. Am. Chem. Soc.* **1978**, *100*, 7894−7900.

(23) Zirong, D.; Bhattacharya, S.; McCusker, J. K.; Hagen, P. M.; Hendrickson, D. N.; Pierpont, C. G. *Inorg. Chem.* **1992**, *31*, 870−877.

(24) Whalen, A. M.; Bhattacharya, S.; Pierpont, C. G. *Inorg. Chem.* **1994**, *33*, 347−353.

(25) Jung, O.-S.; Pierpont, C. G. *Inorg. Chem.* **1994**, *33*, 2227−2235.

(26) Armstrong, W. H.; Lippard, S. J. *Inorg. Chem.* **1985**, *24*, 981−982.

the solid, and the residue was dissolved in pentane. Purple plates crystallized after standing over 6 days at room temperature. Yield: 130 mg (59% based on $H_2$TMRA). FT-IR (KBr, $cm^{-1}$): 3431(br), 2976(s), 2931(w), 2895(vw), 1782(w), 1745(w), 1664(m), 1593-(vw), 1545(vs), 1481(m), 1425(vw), 1394(m), 1365(s), 1294(m), 1225(m), 1146(s), 1078(vs), 985(m), 941(w), 883(m). Anal. Calcd for **1**, $C_{54}H_{74}Cl_2Fe_3O_{18}$: C, 51.90; H, 5.97. Found: C, 51.42; H, 6.24.

**X-ray Crystallographic Study.** Single crystals of **1**·$C_5H_{12}$ were mounted at room temperature on the tips of quartz fibers, coated with Paratone-N oil, and cooled to 123 K under a stream of cold nitrogen maintained by a Bruker LT-2A nitrogen cryostat. Intensity data were collected on a Bruker APEX CCD diffractometer running the *SMART* software package, with Mo K$\alpha$ radiation ($\lambda = 0.71073$ Å). Data collection and reduction protocols are described in detail elsewhere.[27] The structures were solved by direct methods and refined on $F^2$ by using the *SHELXTL* software package.[28] Empirical absorption corrections were applied with the *SADABS* program,[29] an integral part of the *SHELXTL* program package. All non-hydrogen atoms were refined anisotropically, and hydrogen atoms on the methyl groups were assigned idealized positions and given a thermal parameter 1.2 times that of the carbon atom to which they were attached. The hydrogen atom of the O−H functionality of the reduced TMRA ligand was identified on a difference Fourier map and refined.

The pentane molecule in the crystal lattice is located on a general position and has disordered methylene carbon atoms, each of which was modeled at 50% occupancy. Hydrogen atoms were not included in the model. It was difficult to resolve additional pentane molecules, and more than 25% of the crystal comprises disordered solvent, which accounts for the low calculated density. Residual electron density of approximately 1 e/Å$^3$, most likely arising from highly disordered pentane molecules, was not assigned. Final refinement converged at $R = 5.09\%$. The SQUEEZE procedure in *PLATON*[30] was used to approximate the electron density in the void space. The results indicated that, for each molecule of **1**, there are six pentane molecules, five of which are highly disordered. Details of this calculation are supplied in Table S7 of the Supporting Information. Information contained in the main text of this article is based on computations that did not apply SQUEEZE. We also obtained another crystal in the triclinic system that diffracted well enough to reveal the structure, which was refined to $R = 8\%$ and $R_w = 15.1\%$. In this structure, the methyl carbon atoms of the TMRA ligands and the pentane molecules in the lattice were highly disordered.

**Mössbauer Spectroscopy.** The solution sample of **1** used for the Mössbauer study was prepared anaerobically in acetonitrile, transferred to a sample holder by a syringe, and immediately frozen in liquid nitrogen. A Mössbauer study of reactions between ascorbic acid or its anion with iron(II) and iron(III) salts was performed in the following manner. Sample 1 was prepared by dissolving 0.196 g (0.5 mmol) of $(NH_4)_2Fe(SO_4)_2\cdot 6H_2O$ in a 0.1 mM MOPS (MOPS = 4-morpholinepropanesulfonic acid), pH 7.0, aqueous solution (2 mL) under argon. A 0.198 g (1.0 mmol) portion of $Na_2$AA was added with stirring. The solution remained colorless. The flask was opened to air for 5 min, and the air was subsequently removed by several freeze−pump−thaw cycles. An intense purple color developed. The solution was transferred by a syringe into a sample holder and immediately frozen to −78 °C. Sample 2 was prepared in a similar manner by dissolving 0.368 g of $(Et_4N)_2[Fe_2OCl_6]$ in 2 mL of the 0.1 mM MOPS solution. A 0.244 g sample of $Na_2$AA was subsequently added under argon with stirring.

**Table 1.** Conditions for the Redox Titration Experiments

| oxidant | solvent | medium | end-point reading |
|---|---|---|---|
| $(NH_4)_2Ce(NO_3)_6$ in 1.44 M $H_2SO_4$ | $H_2O$ | 1.44 M $H_2SO_4$ | titrator |
| | | 0.576 M $H_2SO_4$ | titrator |
| | | 2.2 M $H_3PO_4$ | *o*-dianisidine |
| | | 0.1 M KCl | titrator |
| | $CH_3CN$ | 0.1 M TBAP | titrator |
| | 50% $CH_3CN/H_2O$ | 0.1 M TBAP | titrator |
| $K_2Cr_2O_7$ in $H_2O$ | $H_2O$ | 0.1% HCl | titrator |
| | | 2.4 M HCl | titrator |
| | | 0.48 M HCl | titrator |
| | | 1.44 M $H_2SO_4$ | titrator |
| $I_2$ with KI in $H_2O$ | $H_2O$ | | starch |

**Redox Titrations of 1.** Redox titrations were employed to assess the assignment of ligand oxidation states in **1**. Table 1 lists all of the oxidants, indicators, solvents, and reaction conditions used for the titrations. The end points were determined by using either a redox indicator or an Orion Research 960 Autochemistry potentiometric titrator equipped with a redox combination electrode (Pt vs Ag/AgCl). All experiments were carried out under an inert atmosphere (nitrogen or argon) at room temperature. In cases where ceric ion or dichromate was used as the oxidant, the system was calibrated by using a primary standard. For the iodometric titration, $I_2$ was prepared as an aqueous $I_3^-$ solution, the concentration of which was determined by using $As_2O_3$ as the primary standard. Titration of free TMRA was always performed as a control to examine the validity of the method employed. For the potentiometric titrations, the studies were usually carried out in 1.44 M aqueous $H_2SO_4$. A three-necked flask was used as the reaction vessel, equipped with a redox combination electrode and an argon gas supply line. The temperature of this system was maintained at 30 °C by using an oil bath. Titrant was added with a Gilson pipetteman (accurate to 0.001 mL).

**Reactivity Studies of 1.** All reactions were carried out at 30 °C in acetone with dried air as the dioxygen source and cyclohexane as the substrate. Methyl benzoate ($1.6 \times 10^{-5}$ M) was used as an internal standard. The reaction was monitored by examining aliquots of the reaction mixture with the use of an HP5890 GC and an HP5971 GC mass spectrometer at periodic time intervals. Three sets of experiments were performed to investigate the ability of **1** to promote the air oxidation of cyclohexane. An in situ system prepared from $(NEt_4)_2[Fe_2OCl_6]$/TMRA was used as the control. (i) A small portion (15−20 mg) of crystalline or microcrystalline **1** was weighed out under dinitrogen and dissolved in acetone. The substrate and standard were added, and the reaction was initiated by opening the solution to air. (ii) A total of 1 equiv of **1** was dissolved in $CH_3CN$ in the drybox, and 7 equiv of acid was added to the purple solution. When $HBF_4\cdot Et_2O$ and *p*-toluenesulfonic acid were added, the color of the solution faded immediately and a white precipitate formed. When benzoic acid was employed, the purple color persisted. The substrate and standard were then added, and the system was exposed to air. (iii) A total of 1 equiv of **1** was dissolved in acetone, and ∼40 equiv of $H_2$TMRA was added to the solution. The system was opened to air after the substrate and standard were added.

---

(27) Kuzelka, J.; Mukhopadhyay, S.; Spingler, B.; Lippard, S. J. *Inorg. Chem.* **2004**, *43*, 1751−1761.

(28) Sheldrick, G. M. *SHELXTL97-2: Program for the Refinement of Crystal Structures*; University of Göttingen: Göttingen, Germany, 1997.

(29) Sheldrick, G. M. *SADABS: Area-Detector Absorption Correction*; University of Göttingen: Göttingen, Germany, 1996.

(30) Spek, A. L. *PLATON, A Multipurpose Crystallographic Tool*; Utrecht University: Utrecht, The Netherlands 2000.

**Table 2.** Summary of X-ray Crystallographic Data for **1**·$C_5H_{12}$

| | $[Fe_3Cl_2(TMRASQ)_4(TMRA)_2]\cdot C_5H_{12}$ (**1**·$C_5H_{12}$) |
|---|---|
| formula | $C_{59}H_{86}Cl_2Fe_3O_{18}$ |
| fw | 1321.75 |
| space group | $I\bar{4}3d$ |
| $a$, Å | 37.4730(4) |
| $V$, Å$^3$ | 52620.6(10) |
| $Z$ | 24 |
| $\rho_{calc}$, g/cm$^3$ | 0.992 |
| $T$, °C | −150 |
| $\mu$(Mo K), mm$^{-1}$ | 0.599 |
| $\theta$ limits, deg | 2.03 − 28.29 |
| total no. of data | 225,261 |
| no. of unique data | 10,869 |
| no. of params | 379 |
| R1[a] | 0.0509 |
| wR2[b] | 0.1483 |
| max, min peaks, e/Å$^3$ | 1.014/−0.422 |

[a] $R1 = \sum||F_o| - |F_c||/\sum|F_o|$. [b] $wR2 = \{\sum[w(F_o^2 - F_c^2)^2]/\sum[w(F_o^2)^2]\}^{1/2}$.

**Table 3.** Selected Bond Lengths and Angles for **1** and Bond Valence Sums for Fe(1) and Fe(2)

| bond[a] | length (Å) | angle (deg) | $\nu_{ij}$ | bond valence sum | average bond length (Å) |
|---|---|---|---|---|---|
| Fe(1)−O(2) | 2.063(3) | | 0.4110 | | |
| Fe(1)−O(2)#1 | 2.063(3) | | 0.4110 | | |
| Fe(1)−O(1) | 2.116(2) | | 0.3561 | 2.048 | 2.139(3) |
| Fe(1)−O(1)#1 | 2.116(2) | | 0.3561 | | |
| Fe(1)−O(3) | 2.237(2) | | 0.2568 | | |
| Fe(1)−O(3)#1 | 2.237(2) | | 0.2568 | | |
| Fe(2)−Cl(1) | 2.2520(9) | | 0.6887 | | |
| Fe(2)−O(3) | 1.906(2) | | 0.6721 | | |
| Fe(2)−O(4) | 1.993(2) | | 0.5313 | | |
| Fe(2)−O(5) | 2.064(2) | | 0.4385 | 3.090 | |
| Fe(2)−O(4)#1 | 2.076(2) | | 0.4245 | | |
| Fe(2)−O(6) | 2.164(2) | | 0.3347 | | |
| Fe(1)−O(3)−Fe(2) | | 114.57(10) | | | |
| Fe(2)−O(4)−Fe(2) | | 104.79(9) | | | |

[a] Symmetry transformations used to generate equivalent atoms: #1, $-x + 1, -y + {}^1/_2, z$.

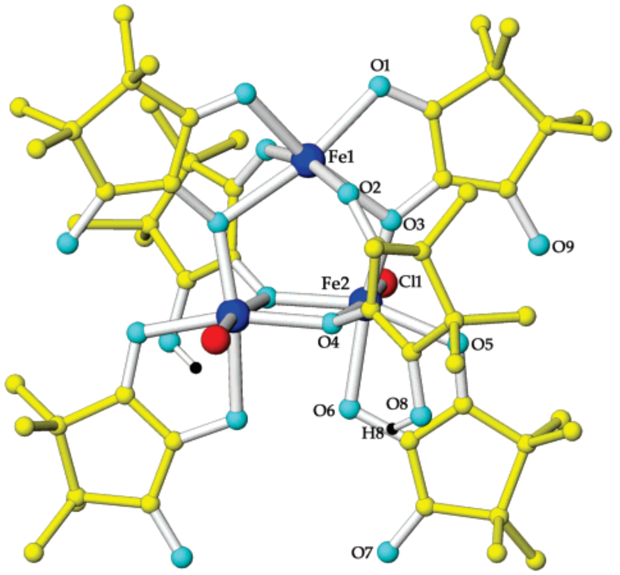

**Figure 1.** Structure of **1**. Iron atoms are blue, carbon atoms yellow, chloride ions red, oxygen atoms blue, and hydroxyl H atoms black. Hydrogen atoms on carbon are omitted for clarity.

## Results and Discussion

**Synthesis, Structural Characterization, and Charge Distribution within $[Fe_3Cl_2(TMRASQ)_4(HTMRA)_2]$.** A proposed reaction scheme for the formation of **1** is shown in eq 1. In support of the reaction stoichiometry, we

$$3(Et_4N)_2[Fe_2OCl_6] + 6H_2TMRA \rightarrow [Fe_3Cl_2(TMRASQ)_4(HTMRA)_2] + 3(Et_4N)_2[FeCl_4] + 4HCl + 3H_2O \quad (1)$$

recovered a large quantity of a green-yellow precipitate that formed during the reaction. The UV−vis spectrum of this material displayed three peaks at 244, 314, and 364 nm, identical to those observed for $(Et_4N)_2[FeCl_4]$.[31]

Crystallographic data for **1** are summarized in Table 2, and selected bond lengths and angles are listed in Table 3. The molecular geometry is depicted in Figure 1. In the structure determined from the cubic crystal data set, three iron atoms in the molecule form an isosceles triangle with a crystallographic 2-fold axis passing through Fe(1) and the center of the Fe(2)···Fe(2)* edge. Consideration of the overall charge of the trinuclear unit (vide infra) necessitates a mixed-valence $Fe^{II}Fe^{III}_2$ assignment; the presence of two ferric and one ferrous ions in the structure was confirmed by Mössbauer spectroscopy, as described below. All three iron atoms in **1** have a distorted octahedral environment. The Fe(1) center has a bond valence sum of 2.048, consistent with an assignment as $Fe^{II}$ (Table 3).[32,33] It is coordinated to six oxygen atoms from four different TMRA ligands. The symmetry-equivalent Fe(2) atoms are also coordinated by four different TMRA ligands and have a terminal chlorine anion. They form an edge-shared bioctahedral substructure comprising two $FeO_5Cl$ units in which there are five Fe−O bonds and one Fe−Cl bond (2.2520(9) Å), the last being somewhat shorter than that in the complex $[FeCl_6]^{3-}$ (∼2.40 Å).[34] The Fe(2)···Fe(2) separation of 3.224 Å in the edge-shared bioctahedral unit is shorter than the two longer, symmetry-related, corner-shared distances Fe(1)···Fe(2) of 3.490 Å.

A detailed analysis of the bond lengths in the three different kinds of ligands in **1** provides insight into their oxidation states, which in turn serves as the basis for a description of the total charge distribution within the complex. It has been demonstrated in the literature[35−37] by consideration of the internal bond lengths for metal catechol complexes that it is possible to assign oxidation states for

---

(31) Day, P.; Jorgensen, C. K. *J. Chem. Soc.* **1964**, 6226−6234.

(32) Thorp, H. H. *Inorg. Chem.* **1992**, *31*, 1585−1588.

(33) Brown, I. D.; Altermatt, D. *Acta Crystallogr.* **1985**, *B41*, 244−247.

(34) Morón, M. C.; Palacio, F.; Pons, J.; Casabó, J.; Solans, X.; Merabet, K. E.; Huang, D. S.; Shi, X.; Teo, B. K.; Carlin, R. L. *Inorg. Chem.* **1994**, *33*, 746−753.

(35) Chaudhuri, P.; Verani, C. N.; Bill, E.; Bothe, E.; Weyhermüller, T.; Wieghardt, K. *J. Am. Chem. Soc.* **2001**, *123*, 2213−2223.

(36) Chlopek, K.; Bill, E.; Weyhermuller, T.; Wieghardt, K. *Inorg. Chem.* **2005**, *44*, 7087−7098.

(37) Kokatam, S.; Weyhermüller, T.; Bothe, E.; Chaudhuri, P.; Wieghardt, K. *Inorg. Chem.* **2005**, *44*, 3709−3717.

**Scheme 4.** TMRA Ligand Coordination Modes

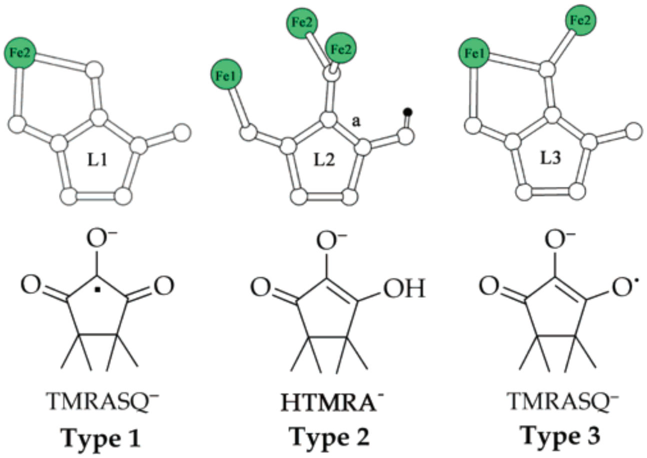

**Table 4.** Selected Bond Lengths for the TMRA Ligand in **1** and Free Reduced $H_2$TMRA

| bond | **L1** | **L2** | **L3** | $H_2$TMRA[a] |
|---|---|---|---|---|
| C−O | 1.368(3) | 1.324(4)<br>1.363(3) | 1.327(4)<br>1.349(3) | 1.318(3)<br>1.363(3) |
| C═O | 1.259(4)<br>1.288(4) | 1.232(4) | 1.239(4) | 1.251(3) |
| C═C | | 1.349(5) | 1.352(4) | 1.345(3) |
| C−C | 1.366(4)<br>1.392(4) | 1.428(4) | 1.424(4) | 1.413(3) |
| type[b] | TMRASQ⁻ | HTMRA⁻ | TMRASQ⁻ | TMRA |

[a] Free $H_2$TMRA data from ref 44. [b] Scheme 4.

**Table 5.** Mössbauer Parameters of Solid and Frozen Acetonitrile Solution Samples of **1** at 80 K and Zero Magnetic Field

| sample | site | $\delta$ (mm/s) | $\Delta E_Q$ (mm/s) | % |
|---|---|---|---|---|
| solid | $Fe^{II}$ | 1.297 | 2.752 | 30 |
| | $Fe^{III}$ | 0.525 | 0.480 | 70 |
| solution | $Fe^{II}$ | 1.297 | 2.742 | 31 |
| | $Fe^{III}$ | 0.534 | 0.550 | 69 |

the ligands. Such is also the case here. Charge distributions within the TMRA ring can be characterized by an analysis of bond distances (Scheme 4), and we summarize our assignments in Table 4. In the fully reduced ligand (type 2), the C═C bond of the enediol fragment, corresponding to **a** in **L2** (Scheme 4), is shorter than the corresponding distance in the type 1 semiquinone form due to the different electron density distribution in the two redox states. The carbon−carbon distance for the C═C double bond in the five-membered chelate ring of **L3** is similarly shortened (Table 4). The carbon−oxygen bond (C═O) in **L2** is 1.232(4) Å, a value that is expected for a double bond. The corresponding bonds in **L1** and **L3** are similarly short. The electronic structures of complexes containing unsaturated five- or six-membered rings have been investigated,[38−41] and a correlation between the structure and ligand charge has been established[42] in a survey of complexes containing quinone-based ligands. The semiquinone forms of the ligand generally have C−O distances that are close to 1.28 Å, and bridging ligands of both types generally have C−O bond lengths that are slightly larger than these normal values, as is apparent in the structure of the [Fe(DBSQ)(DBCat)]$_4$ tetramer.[43] The coordinated C−O single bond lengths average 1.34 Å, similar to the average value of the corresponding distances in fully reduced $H_2$TMRA,[44] which is included for comparison purposes in Table 4. The C−O bond of the peripheral hydroxyl group in free $H_2$TMRA is shorter than that of the central group.[44]

The foregoing assignment of TMRA oxidation levels is consistent with the six ligands carrying a total of six negative charges, resulting in an overall neutrality of **1**. As discussed above, both the fully reduced and semiquinone forms of the ligand (Scheme 4) are involved. The iron atoms contribute a total of eight positive charges, the chloride ions two negative charges, and the TMRA ligands a total of six negative charges. There are two possible TMRA combinations that satisfy this requirement: (i) six monoanionic ligands or (ii) two neutral, two monoanionic, and two dianionic ligands. The former is the more reasonable combination both to satisfy the results of the redox titration (see below) and to avoid asymmetric charge localization among an otherwise quite similar set of ligands. We therefore conclude that, as indicated in Scheme 4, there are six monoanionic ligands, of which four are TMRASQ⁻ monoanions and two are HTMRA⁻ monoanions. The protons of the latter were readily resolved on difference Fourier electron density maps in the structure determination and satisfactorily refined.

Three different types of TMRA coordination modes occur in **1**. Two TMRA ligands coordinate in a bidentate, chelating fashion to only one iron atom (**L1** in Scheme 4), two bridge three metal atoms in a bidentate mode (**L2**), and two link two different iron atoms in a mixed chelating/bridging manner (**L3**). All three of these binding patterns have been previously observed in a tetranuclear iron complex with 3,5-di-*tert*-butyl-1,2-benzoquinone as the ligand.[43] An intermolecular hydrogen-bonding network exists in the crystal structure of **1** (Figure 2). The terminal hydroxyl groups of the two **L2** ligands donate hydrogen atoms to the non-coordinating oxygen atoms of TMRASQ in another molecule to form strong intermolecular hydrogen bonds having an O8−H8···O7 distance of 2.658 Å and an interbond angle of 157.15°.

Compound **1** is the first example of an iron complex bound to ascorbate or one of its analogues to be structurally characterized. The corresponding iron AA complex is likely to be quite similar. Ascorbate is capable of forming chelates like TMRA, and an iron ascorbate complex with a structure similar to that of **1** would be consistent with observations obtained from previous Mössbauer and spectroscopic stud-

---

(38) McCleverty, J. A. *Prog. Inorg. Chem.* **1968**, *10*, 49−221.

(39) Attia, A. S.; Bhattacharya, S.; Pierpont, C. G. *Inorg. Chem.* **1995**, *34*, 4427−4433.

(40) Jung, O.-S.; Pierpont, C. G. *J. Am. Chem. Soc.* **1994**, *116*, 2229−2230.

(41) Jung, O.-S.; Pierpont, C. G. *J. Am. Chem. Soc.* **1994**, *116*, 1127−1128.

(42) Carugo, O.; Castellani, C. B.; Djinovic, K.; Rizzi, M. *J. Chem. Soc., Dalton Trans.* **1992**, 837−841.

(43) Boone, S. R.; Purser, G. H.; Chang, H.-R.; Lowery, M. D.; Hendrickson, D. N.; Pierpont, C. G. *J. Am. Chem. Soc.* **1989**, *111*, 2292−2299.

(44) Feng, X.; Bott, S. G.; Lippard, S. J. *Acta Crystallogr.* **1990**, *C46*, 1671−1674.

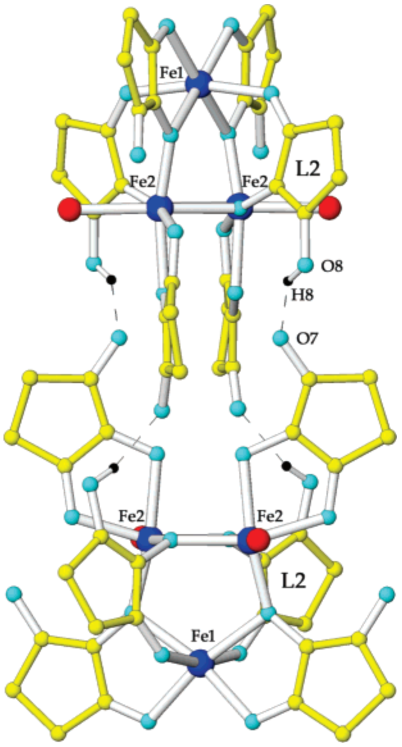

**Figure 2.** Two molecules of **1** in the crystal structure showing the hydrogen-bonding network. Terminal methyl groups on the TMRA ligands are omitted for clarity.

**Scheme 5**

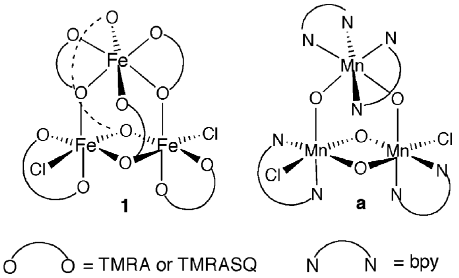

ies.[45] The core geometry of **1** is unique among the trinuclear iron clusters with oxygen bridges. Among the known trinuclear iron clusters, the most common structural motif is that of the basic iron acetate, which contains an equilateral triangular array of iron atoms. This core distorts toward an isosceles triangle when one of the iron atoms is reduced to the ferrous form. The trinuclear iron(III) complex $[Fe_3O(TIEO)_2(O_2CPh)_2Cl_3]_2 \cdot C_6H_6$ (TIEOH = 1,1,2-tris(*N*-methyl-2-imidazolyl)ethanol) also has an isosceles triangular core.[46] A trinuclear mixed-valent iron complex, $[Fe_3O(OAc)_6(TACN)] \cdot 2CHCl_3$ (TACN = 1,4,7-triazacyclononane), has been characterized, with an isosceles triangular core different from that of the classical mixed-valent basic iron acetate.[47] All of these complexes have a $\{Fe_3O\}^{6+,7+}$ unit with only small variations in their core geometry from that of the basic iron acetate. In addition, a number of linear trinuclear iron clusters have appeared in the literature.[48,49] Among the iron

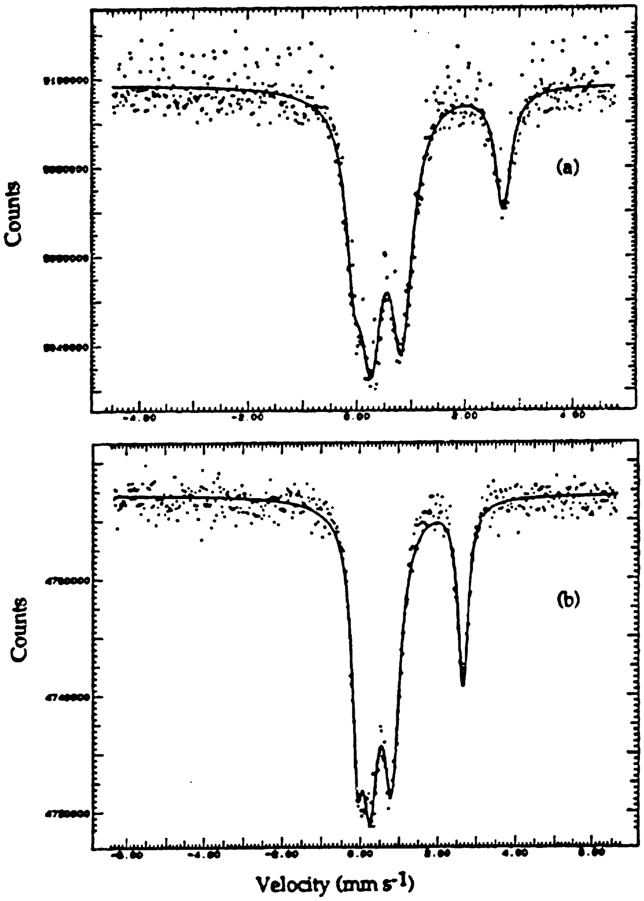

**Figure 3.** Zero-field Mössbauer spectra at 80 K for (a) solid and (b) acetonitrile solution samples of **1**. The solid lines are the least-squares fits to the data.

complexes with a triangular structural motif, complex **1** provides the sole example of a core geometry with only alkoxo bridges. The double alkoxide bridge between the Fe(2) and Fe(2) atoms observed in **1** is also uncommon among the trinuclear iron clusters.

Many of the structural features of **1** are shared by the trinuclear manganese complex $[Mn_3O_4(bipy)_4X_2]^{n+}$ (X = Cl, $n = 2$, **a**; X = $H_2O$, $n = 4$, **b**) (Scheme 5).[50,51] As depicted in Scheme 5, complex **a** has a triangular metal cluster similar to that observed in **1** but with oxo rather than alkoxo bridges between metal centers. Two $C_2$-symmetry-related chloride ions occupy terminal positions at the base of the triangles in the two structures. The trimanganese analogue **b**, in which the two chloride ligands are replaced by two water molecules, is an active catalyst for hydroxylating alkanes with the use of $^t$BuOOH as the oxidant.[52,53]

---

(45) Lynch, S. R.; Cook, J. D. *Ann. N. Y. Acad. Sci.* **1980**, *355*, 32−44.
(46) Gorun, S. M.; Papaefthymiou, G. C.; Frankel, R. B.; Lippard, S. J. *J. Am. Chem. Soc.* **1987**, *109*, 4244−4255.
(47) Poganiuch, P.; Liu, S.; Papaefthymiou, G. C.; Lippard, S. J. *J. Am. Chem. Soc.* **1991**, *113*, 4645−4651.
(48) Rardin, R. L.; Bino, A.; Poganiuch, P.; Tolman, W. B.; Liu, S.; Lippard, S. J. *Angew. Chem., Int. Ed. Engl.* **1990**, *29*, 812−814.
(49) Chen, X.-D.; Du, M.; He, F.; Chen, X.-M.; Mak, T. C. W. *Polyhedron* **2005**, *24*, 1047−1053 and references cited therein.
(50) Auger, N.; Girerd, J.-J.; Corbella, M.; Gleizes, A.; Zimmermann, J.-L. *J. Am. Chem. Soc.* **1990**, *112*, 448−450.
(51) Sarneski, J. E.; Thorp, H. H.; Brudvig, G. W.; Crabtree, R. H.; Schulte, G. K. *J. Am. Chem. Soc.* **1990**, *112*, 7255−7260.
(52) Sarneski, J. E.; Michos, D.; Thorp, H. H.; Didiuk, M.; Poon, T.; Blewitt, J.; Brudvig, G. W.; Crabtree, R. H. *Tetrahedron Lett.* **1991**, *32*, 1153−1156.
(53) Dziobkowski, C. T.; Wrobleski, J. T.; Brown, D. B. *Inorg. Chem.* **1981**, *20*, 679−684.

**Scheme 6**

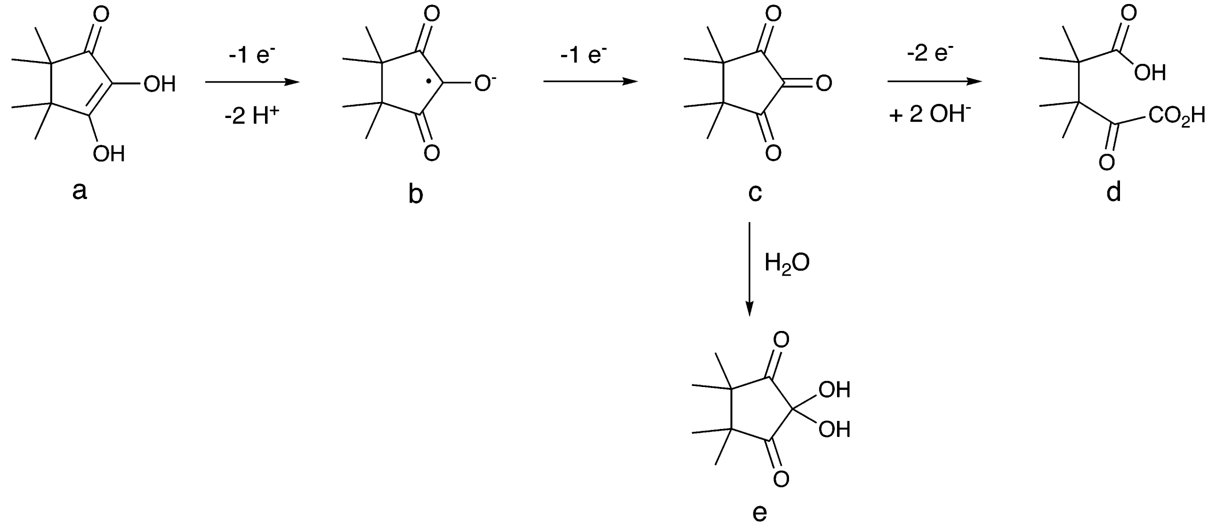

**Table 6.** Results from the Redox Titrations of Free TMRA and **1**

| oxidant | solvent/medium | end point | $H_2TMRA$ | **1** |
|---|---|---|---|---|
| $(NH_4)_2Ce(NO_3)_6/0.72$ N $H_2SO_4$ | $H_2O/2.2MH_3PO_4$ | *o*-dianisidine | 1.93 | 10.7, 9.9 |
| | | | 2.00, 2.00 | 8.4, 8.2 |
| | $CH_3CN/0.1$ M TBAP | titrator | 1.91, 1.93 | |
| $K_2Cr_2O_7$ in $H_2O$ | $H_2O/10\%$ HCl | titrator | 2.03, 2.09 | |
| $I_3^-$ | $H_2O$ | starch | 1.97, 1.95 | 9.1, 9.9 |

**Mössbauer Studies.** Figure 3 shows the Mössbauer spectra of solid and frozen solution samples of **1** at 80 K in zero magnetic field. The fitting parameters are listed in Table 5. Spectra taken at different temperatures showed very little temperature dependence. The iron atoms are in two chemically different sites. The isomer shifts of the two sites are typical of those for high-spin $Fe^{II}$ and $Fe^{III}$, with a relative $Fe^{II}/Fe^{III}$ ratio of 1:2. The values are comparable to those in other high-spin $Fe^{II}$ and $Fe^{III}$ complexes.[54] To examine the integrity of **1** in solution, a solution spectrum was taken. Both Mössbauer parameters ($\delta$ and $\Delta E_Q$), as well as the ratio of ferric to ferrous ion, were very similar to that observed for the solid sample. This result is consistent with **1** having a similar structure in both the solid and solution states.

**Redox Titration Studies.** $H_2TMRA$ can be oxidized under appropriate conditions to form $1e^-$, $2e^-$, and $4e^-$ oxidation products, as shown in Scheme 6.[55] Under the proper titration conditions, the oxidation of **1** can be halted at a given stage. By determination of the number of redox equivalents required to oxidize all ligands in **1** to a certain oxidation state, for example, the triketone form, the redox states of the ligands in **1** can in principle be assigned. There were two major difficulties encountered in carrying out such a titration, using a $Ce^{4+}$ ion as the oxidant in a 0.72 N $H_2SO_4$ aqueous solution and *N*-phenylanthranilic acid as the indicator. First, the end point was not stable, possibly due to reaction between TMRA and the indicator. When $H_2TMRA$ was titrated, the clear solution became cloudy upon the addition of a few drops of the indicator solution. To circumvent this problem, a different indicator, *o*-dianisidine, was employed, which generates a stable and distinctive orange color at the end point. The use of the potentiometric titration methodology also avoided the aforementioned problem by eliminating the need for indicators altogether. Second, the results obtained were irregular and not reproducible. Further oxidation of the triketone by the strong oxidant $Ce^{4+}$ was suspected. The use of a milder oxidant, $I_2$, alleviated this problem, and $I_2$ has been used to quantitate $H_2TMRA$ in the literature by oxidizing the fully reduced form exclusively to the triketone (Scheme 6).[56] The titration results for both $H_2TMRA$ and **1** are reported in Table 6. The total number of oxidation equivalents required to titrate the ligands in 1 equiv of **1** is $9 \pm 1$, which is consistent with the oxidation of two fully reduced $H_2TMRA$ ligands ($4e^-$), four semiquinone ligands ($4e^-$), and one ferrous ion ($1e^-$). This result is in agreement with the assignments of the X-ray crystal structure determination and the Mössbauer spectrum.

**Reactivity of 1.** The role of **1** in the catalytic hydroxylation of alkanes by dioxygen is of interest. To discuss this topic effectively, we first briefly recount the nature of the in situ catalytic system, a detailed description of which was published elsewhere.[19] In a typical in situ catalytic reaction, $(Et_4N)_2[Fe_2OCl_6]$ is employed, together with a 20-fold excess of TMRA as the reductant. When cyclohexane is used as a substrate, 3.5 mol of cyclohexanol and less than 0.08 mol of cyclohexanone per 1 mol of $(Et_4N)_2[Fe_2OCl_6]$ are formed (~17% based on the reductant) in only 5 h at 32 °C. The addition of a second portion of the reductant affords an additional 70−80% of original activity after another 5 h.

The catalytic reactivity of **1** toward hydroxylation of alkanes is significantly different from that of the in situ system, however, especially with respect to selectivity. The

---

(54) Tshuva, E. Y.; Lippard, S. J. *Chem. Rev.* **2004**, *104*, 987−1012.

(55) Inbar, S.; Ehret, A.; Norland, K. *Abstracts of Papers*; National Meeting of the Society of Photographic Sciences, Minneapolis, MN, 1987.

(56) Hesse, G.; Wehling, B. *Liebigs Ann. Chem.* **1964**, *679*, 100−106.

catalytic activity of **1** in the air oxidation of cyclohexane was examined by using (i) only **1** and $O_2$; (ii) **1**, acid, and $O_2$; and (iii) **1**, extra $H_2$TMRA, and $O_2$. In the presence of **1** alone (i), conversion of cyclohexane to cyclohexanol is very slow. Cyclohexanol was formed with an overall yield of about 42% based on the complex and an alcohol/ketone ratio of 1.9:1 over 24 h. The addition of excess protons accelerated the oxidation reaction slightly and gave a total yield of 52%. In the presence of excess $H_2$TMRA, complex **1** catalyzed the oxidation reaction with a rate and overall yield comparable to those found in the in situ system.[19] However, the selectivity toward the formation of cyclohexanol, with a 7:1 cyclohexanol/cyclohexanone ratio in the oxidation products, is much lower than that for the in situ system. This result suggests that **1** is actively involved in the catalytic cycle but that it is not the sole active species that is responsible for the catalytic reactivity and selectivity of the in situ system.

An attempt to investigate the kinetics of hydrocarbon oxidation by **1** and dioxygen revealed the presence of a lag period following initiation of the reaction, strongly suggesting that **1** is not the true catalyst but a precursor to the active species.[57] This finding launched our subsequent studies of carboxylate-bridged diiron complexes as structural and functional models of bacterial multicomponent monooxygenases, reviewed elsewhere.[54,58,59]

**Mössbauer Studies of the Ascorbate Analogue of 1.** It is very difficult to prepare and crystallize the ascorbate analogue of **1** from nonaqueous solvents owing to the limited solubility of ascorbic acid. The formation of a purple complex between ferrous sulfate and ascorbic acid (eq 2a) was observed in aqueous solution, but the lifetime of the complex was quite short; at room temperature the color bleached within a few minutes. Attempts to crystallize a complex formed between an iron salt and ascorbic acid have not succeeded to date. A solution Mössbauer study was therefore undertaken to offer some insight into the nature the complex. The pH of the medium was determined to be

$$(NH_4)_2Fe(SO_4)_2 + AA \xrightarrow{aq} \text{colorless} \xrightarrow{O_2} \text{purple} \quad (2a)$$

$$(NH_4)_2Fe(SO_4)_2 + 1.5NaAA \xrightarrow{pH\ 7} \text{colorless} \xrightarrow{O_2,\ 5\ min} \text{purple} \quad (2b)$$

$$(NEt_4)_2[Fe_2OCl_6] + 2NaAA \xrightarrow{pH\ 7,\ Ar} \text{purple} \quad (2c)$$

crucial for stabilizing the complex. At pH 7, the purple complex lasted for about 1 h in air and was stable indefinitely in the absence of air. A 0.1 mM solution of monosodium ascorbate (NaAA) was prepared in MOPS buffer to maintain the pH of the solution at 7. Samples prepared according to eqs 2b and 2c were frozen at −78 °C, and their Mössbauer spectra were recorded. The derived Mössbauer parameters listed in Table 7 clearly indicate the presence of a mixed-valent species. Differences in the $Fe^{II}/Fe^{III}$ ratio between the various preparations may be a consequence of incomplete oxidation of the sample prepared via the route of eq 2b. The UV−vis spectrum of the solution prepared according to eq 2c showed a peak at 475 nm and a shoulder at 550 nm. It is interesting to note that the $Fe^{II}/Fe^{III}$ ratio of >1 is just the opposite of what was observed in complex **1**. The result obtained by method 2b is very similar to that reported for the purple complex formed upon exposure of a $FeCl_2{\cdot}4H_2O$ and 10-fold NaAA mixture to dioxygen, which has a ferrous-to-ferric ion ratio of 3:1. The existence of excess reductant seems to have little effect on the Mössbauer properties of the iron centers and the relative ratio of $Fe^{II}/Fe^{III}$ in the complex.

**Table 7.** Mössbauer Parameters for Solution Samples of the Ascorbate Analogue of **1**

| | $Fe^{II}$ | | | $Fe^{III}$ | | |
|---|---|---|---|---|---|---|
| sample | $\delta$ (mm/s) | $\Delta E_Q$ (mm/s) | % | $\delta$ (mm/s) | $\Delta E_Q$ (mm/s) | % |
| $Fe_2OCl_6$ + 2NaAA | 1.390 | 3.246 | 66.8 | 0.513 | 0.613 | 33.2 |
| $Fe^{2+}$ + 1.5NaAA + $O_2$ | 1.364 | 3.135 | 74.4 | 0.523 | 0.522 | 25.6 |
| $Fe^{2+}$ + 10NaAA + $O_2$ | 1.34 | 2.94 | 77 | 0.36 | 0.29 | 23 |

## Conclusions

A novel trinuclear mixed-valent iron TMRA complex, **1**, was isolated and structurally characterized. The molecule has a unique core geometry, with three iron atoms, one ferrous and two ferric, forming an isosceles triangle. The oxidation states of the ligands were determined by detailed bond length analysis and redox titrations to be two fully reduced and four semiquinone TMRA ligands. Two chloride ions, coordinated to two of the $Fe^{III}$ centers, complete the octahedral coordination spheres and may delineate possible coordination sites for dioxygen binding and activation in the catalytic chemistry.

As the first structurally characterized iron complex of an ascorbate analogue, the structure of **1** provides considerable insight into the possible coordination geometry of iron AA complexes. A Mössbauer study of a solution sample containing a purple iron AA complex prepared at pH 7 indicates the existence of a multinuclear mixed-valent cluster.

Complex **1** promotes interesting reactivity, the selective air oxidation of cyclohexane. In the presence of **1** alone, the yield of the product formation reached as high as 42% based on the complex but was less selective for the formation of alcohol versus ketone (1.9:1) than for that of an in situ catalytic system based on $(Et_4N)_2[Fe_2OCl_6]$, $O_2$, and $H_2$TMRA. The addition of excess acid improved the yield slightly to 52%, while the addition of excess $H_2$TMRA gave similar yields (14% based on the reductant) compared to the system prepared in situ. These results suggest that a species similar to **1** is involved in the catalytic cycle, either directly or indirectly. It is likely based on preliminary kinetic data that **1** acts as a precursor from which the real active species is generated. The catalytically active species,

---

(57) Feig, A. L.; Lippard, S. J. Unpublished results.

(58) Du Bois, J.; Mizoguchi, T. J.; Lippard, S. J. *Coord. Chem. Rev.* **2000**, *200−202*, 443−485.

(59) Feig, A. L.; Lippard, S. J. *Chem. Rev.* **1994**, *94*, 759−805.

most likely an activated oxygenating agent, can be generated by coordinating dioxygen to one of the iron atoms after the dissociation of labile ligand chloride. Further work would be required to delineate the details of this interesting system.

**Acknowledgment.** This work was supported by grants from the National Science Foundation and the National Institutes of Health. Y.K. thanks the Korea Research Foundation Grant funded by the Korea Government for a postdoctoral fellowship. We are grateful to Dr. Georgia C. Papaefthymiou of the Francis Bitter National Magnet Laboratory for assistance with recording and analysis of the Mössbauer spectra and to Dr. Lloyd Taylor of Polaroid Corp. for a generous gift of $H_2$TMRA.

**Supporting Information Available:** Crystal data and structure refinement, atomic and hydrogen coordinates, isotropic and anisotropic displacement parameters, and bond lengths and angles for **1**. This material is available free of charge via the Internet at http://pubs.acs.org.

IC700622A